Rearrangement-Free Hydroxylation of Methylcubanes by a Cytochrome P450: The Case for Dynamical Coupling of C–H Abstraction and Rebound

Md. Raihan Sarkar,[†,§,^] Sevan D. Houston,[‡,§] G. Paul Savage,[¶] Craig M. Williams,[*,‡] Elizabeth H. Krenske,[*,‡] Stephen G. Bell[*,†] and James J. De Voss[*,‡]

[†]Department of Chemistry, University of Adelaide, Adelaide, SA 5005, Australia; [‡]School of Chemistry and Molecular Biosciences, University of Queensland, Brisbane, QLD 4072, Australia; [¶]CSIRO Manufacturing, Ian Wark Laboratory, Melbourne, VIC 3168, Australia.

ABSTRACT: The highly strained cubylmethyl radical undergoes one of the fastest radical rearrangements known (reported $k = 2.9 \times 10^{10}$ s^{-1} at 25 °C) through scission of two bonds of the cube. The rearrangement has previously been used as a mechanistic probe to detect radical-based pathways in enzyme-catalyzed C–H oxidations. This paper reports the discovery of highly selective cytochrome P450-catalyzed methylcubane oxidations which notionally proceed via cubylmethyl radical intermediates yet are remarkably free of rearrangement. The bacterial cytochrome P450 CYP101B1 from *Novosphingobium aromaticivorans* DSM 12444 is found to hydroxylate the methyl group of a range of methylcubane substrates containing a regio-directing carbonyl functionality at C-4. Unlike other reported P450-catalyzed methylcubane oxidations, the designed methylcubanes are hydroxylated with high efficiency and selectivity, giving cubylmethanols in yields of up to 93%. The lack of cube ring opening implies that the cubylmethyl radicals formed during these CYP101B1-catalyzed hydroxylations must have very short lifetimes, of just a few picoseconds, which are too short for them to manifest the side reactivity characteristic of a fully equilibrated P450 intermediate. We propose that the apparent ultrafast radical rebound can be explained by a mechanism in which C–H abstraction and C–O bond formation are merged into a dynamically coupled process, effectively bypassing a discrete radical intermediate. Related dynamical phenomena can be proposed to predict how P450s may achieve various other modes of reactivity by controlling the formation and fate of radical intermediates.In principle, dynamical ideas and two-state reactivity are each individually able to explain apparent ultrashort radical lifetimes in P450 catalysis, but they are best considered together.

INTRODUCTION

The ability of cytochrome P450s to carry out a range of difficult chemical transformations has driven intense activity across many disciplines of chemistry seeking to uncover, understand, and engineer new realms of P450 reactivity.[1] Studies of new P450–substrate pairings shed important new light on the details of these enzymes' complex catalytic mechanisms.[2]Chemical probes, in particular strained hydrocarbon substrates, have played an important role in determining the involvement of radical intermediates and the timing of the bond forming and breaking processes.[3,4]

This paper reports novel mechanistic insights which emanate from unexpected behavior observed in P450-catalyzed oxidations of methylcubanes. Cubane itself is a highly strained but metabolically stable hydrocarbon[5] which has recently been introduced as a benzene bioisostere in drugs and agrichemicals.[6] These applications are possible because the strong C–H bonds of cubane (similar in strength to a benzene C–H bond)[5a,6c,7]give it a low susceptibility to P450-mediated oxidative drug metabolism. Conversely, derivatives of methylcubane (**1**) are susceptible to enzymatic degradation, including by P450s. Putative intermediates in different enzyme-catalyzed oxidations of **1** include – formally at least – the cubylmethyl cation and radical, both of which are known to undergo rapid skeletal rearrangements when generated chemically (Scheme 1). An incipient cubylmethyl cation **3** is implicated in the acid-catalyzed rearrangement of cubylmethanol **2** to homocubanol **5** (via **4**); in this rearrangement, a 1,2-carbon–carbon bond migration leads to the expansion of one edge of the cube.[6a] In contrast, the cubylmethyl radical **7**, generated by photolysis of precursor **6**, rearranges via scission of two or more of the cube C–C bonds to give ladderene (**9**) and bis-cyclobutenyl (**10**) radicals.[7,8] The first two β-scission steps in the rearrangement of **7** are among the fastest radical rearrangements known, with rate constants of 2.9×10^{10} s^{-1} and $>1.5 \times 10^{11}$ s^{-1} at 25 °C.[8b]

Scheme 1. Distinct reactivities of methylcubane derivatives in cationic *versus* radical manifolds

1

(a) Cationic rearrangement

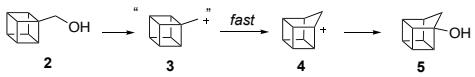

2 **3** **4** **5**

(b) Radical rearrangement

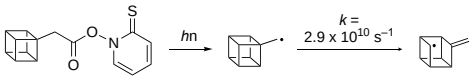

6 **7** **8**

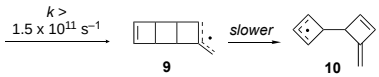

9 **10**

Scheme 2. Reported products of oxidations of methylcubane (1) by various MMO and cytochrome P450 enzymes

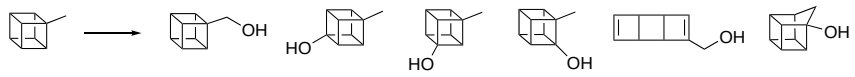

1 **2** **11** **12** **13** **14** **5**

MMO *M. cap.*[b,d]	100%	0% total methylcubanols			0%	0%
MMO *M. tri.*[e]	40%	18% total methylcubanols			42%[c]	0%
CYP2B1[b,d]	22%	38%	29%	13%	nr	nr
CYP2B1[b,f]	54–78%	5–17%	6–19%	9–17%	0%	<1%
CYP2E1[b,f]	42–71%	10–20%	7–20%	1–13%	0%	6–14%

[a]*M. cap*: *Methylococcus capsulatus* (Bath), *M. tri*.: *Methylosinus trichosporium* OB3b, CYP: cytochrome P450. [b]Products were derivatized as acetates. [c]Later reassigned[10a]as **5**. [d]Ref. 9. [e]Ref. 10b. [f]Ref. 10a.nr: not reported. The total yields of products in these examples were low: <25 μmoles total product or <1% yield reported for the CYP and*M. cap.*MMO reactions; ca. 5% yield for the *M. tri.* MMO reaction.

These fast rearrangements, and their distinctive products, have enabled methylcubane to be used as a mechanistic probe substrate to distinguish between cationic and radical pathways in enzyme-catalyzed C–H oxidation reactions.8[d,9,10]The oxidations of methylcubane by methane monooxygenase (MMO) and mammalian cytochrome P450 enzymes have been studied in detail. Key examples are shown in Scheme 2. The percentages listed in Scheme 2 represent product distributions rather than yields. The oxidation of methylcubane by the MMO from *Methylococcus capsulatus* (Bath) yielded solely cubylmethanol **2**, derivatized as the acetate for analysis.9 In contrast, the oxidation of methylcubane by the MMO from *Methylosinus trichosporium* OB3b gave a mixture of cubylmethanol **2** (40%), methylcubanols **11**–**13** (18%), and a "radical rearrangement product" assigned as ladderene **14** (42%).[10b] A subsequent report[10a] suggested that the "radical rearrangement product" was in fact not ladderene **14** but homocubanol **5**, which would have likely been derived via a cationic pathway.

In the cytochrome P450-catalyzed reactions, mixtures of products were obtained, comprising cubylmethanol **2**, methylcubanols **11**–**13**, and sometimes homocubanol **5**.[10]Most mammalian P450 systems used in these studies are known to have spacious substrate binding pockets that would allow the substrate to bind in multiple different orientations, explaining the low regioselectivities. Likewise, the contrasting regioselectivities displayed by the two MMOs in Scheme 2 can be attributed to the larger substrate binding pocket of the *M. trichosporium* enzyme as compared with the *M. capsulatus* MMO.[10b] The contrasting results of the MMO and P450 methylcubane oxidations can be further rationalized in terms of the different reactive intermediates (non-heme versus heme iron) and degrees of substrate specificity of each system (small-substrate specific MMO versus promiscuous P450).[9,10]

In all of these reported P450 methylcubane oxidations, the turnover rates and yields of oxidized products were very low (<1%). This, together with the volatilities of the reactant and products, meant that the product mixtures could not easily be quantified with accuracy. Hence, a definitive conclusion about the mechanism(s) of methylcubane oxidation could not be reached. Thisremains an unresolved problem, especially for P450-catalyzed oxidations which appear to yield both radical- and cation-derived products.

The prevailing mechanistic understanding of P450-catalyzed hydroxylations is centered on a radical rebound mechanism.[3] In the classic rebound picture, a hydrogen atom is abstracted from the substrate by an iron-oxo oxidant (Cpd I) to give an intermediate carbon-centered radical.3[a–d] The radical then rebounds by recombining with the Fe(OH) group to give the product Fe–alcohol complex. A key piece of evidence supporting the involvement of radical intermediates in these reactions is the detection of rearranged products of definite radical-based origin; for example, the oxidation of norcarane involves a cyclopropylcarbinyl radical ring opening, **I→II**. These rearrangements, with known (chemically determined) rate constants, have been used as clocks to quantify the rate constants for P450 rebound processes.4

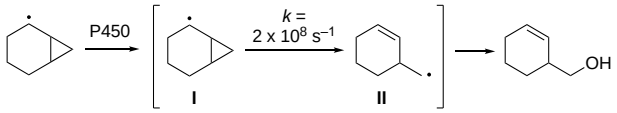

This paper reports the discovery of the first high-yielding cytochrome P450-catalyzed methylcubane oxidations. These reactions ostensibly proceed via cubylmethyl radical intermediates yet remarkably show no evidence for any skeletal rearrangement. The reactions involve the bacterial cytochrome P450 CYP101B1 from *Novosphingobium aromaticivorans* DSM 12444, which is found to selectively hydroxylate the methyl group of a series of methylcubane substrates containing a directing group at the C-4 position relative to methyl. The unexpectedly selective hydroxylations appear to indicate an ultrafast rebound process. Rationalization of these results leads to the proposal that a full understanding of P450 catalysis must take into account not only the well-known contributions of different spin states, but also the dynamics of the bond forming and breaking events. In this picture, the lifetime of the radical "intermediate" depends on the extent of dynamical coupling of the C–H abstraction and C–O bond-forming processes, which may be so closely separated in time that the intermediate is bypassed entirely, or nearly so.

RESULTS AND DISCUSSION

Substrate design and synthesis. Our previous work demonstrated that C–H oxidations catalyzed by the *N. aromaticivorans* CYP101B1 were more efficient and selective when the substrate incorporated a carbonyl substituent.[11] For example, α-ionone, isobornyl acetate, cyclooctyl acetate, and 2-adamantyl acetate were each oxidized at a C–H bond distal to the carbonyl-containing substituent. Although a crystallographic structure of CYP101B1 is not yet available, this regio-control presumably involves a specific interaction between the carbonyl functionality and one or more hydrogen bond donors in the CYP101B1 active site. In the present work, the six methylcubane substrates **15**–**20** (Table 1) were designed and synthesized, each possessing a carbonyl-containing functionality at the C-4 position of the cubane ring system to promote oxidation at the methyl group (or substituted methyl group in the case of **20**). Substrates **15**–**19** were produced from cubane-1,4-dicarboxylic acid, while **20** was synthesized from the corresponding monomethyl ester (see Schemes S2 and S3 of the Supporting Information).

Enzyme assays and identification of products. The results of *in vitro* assays of substrate binding (via heme iron spin state shift assays) and catalytic turnover of **15**–**20** by the *N. aromaticivorans* CYP101B1 enzyme are shown in Table 1, Figure 1, and Figures S1–S3. Substrates **17**–**20** induced a ≥50% shift of CYP101B1 to the high spin form, indicating a good fit between these substrates and the active site. Substrate **15** induced a smaller shift, whereas **16** did not alter the spin state appreciably. The ethylcubane derivative **20** produced a more extensive shift of the CYP101B1 spin state compared with methyl analogue **18**.

Table 1. Substrate binding, turnover and coupling efficiency data for the CYP101B1 catalyzed oxidation of methylcubane derivatives.[a]

CYP101B1 Substrate	%HS heme	NADH oxidation rate	Product formation rate	Coupling (%)
 (**15**)	30	251 ± 10	< 10	< 5
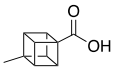 (**16**)	<5	39[b]	nd	nd
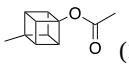 (**17**)	60	374 ± 10	< 10	< 2.5
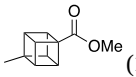 (**18**)	50	446 ± 5	296 ± 29	66
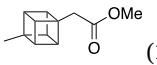 (**19**)	85	468 ± 7	189 ± 35	41
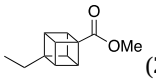 (**20**)	70	690 ± 28	298 ± 32	43

Turnover activities were measured using a ArR:Arx:CYP101B1 concentration ratio of 1:10:1 (0.5 μM CYP enzyme, 50 mM Tris, pH 7.4). (ArR and Arx are the protein redox partners required for CYP101B1 activity.[11d–g]) Rates are reported as the mean ± S.D. (n ≥ 3 unless otherwise noted) and are given in nmol.nmol-CYP^{-1}.min^{-1}. The coupling is the percentage of consumed NADH utilized for the formation of products. nd: not determined due to lack of product formation. [b]Measured by a single experiment.

Little or no product was detected in enzyme turnover assays of **15**, **16**, or of **17**. The latter result was unexpected, given the significant spin state change induced by binding of **17** to CYP101B1. By contrast, the oxidations of the better matched substrates **18**–**20** each gave significant quantities of a single major product, corresponding to a regioselectively monooxygenated species, as detected by GC and GC-MS analysis. The rates of product formation varied from 189 to 298 nmol.nmol-CYP^{-1}.min^{-1}. The coupling efficiencies (i.e. the proportion of consumed NADH reducing equivalents utilized for the formation of oxygenated products) were good, ranging from 41 to 66%. These rates and efficiencies are comparable to those previously observed for CYP101B1 with carbonyl-substituted adamantanes and norisoprenoids, which displayed rates of 166–1350 nmol.nmol-CYP^{-1}.min^{-1} and coupling efficiencies of 48–99%.[11d–f]

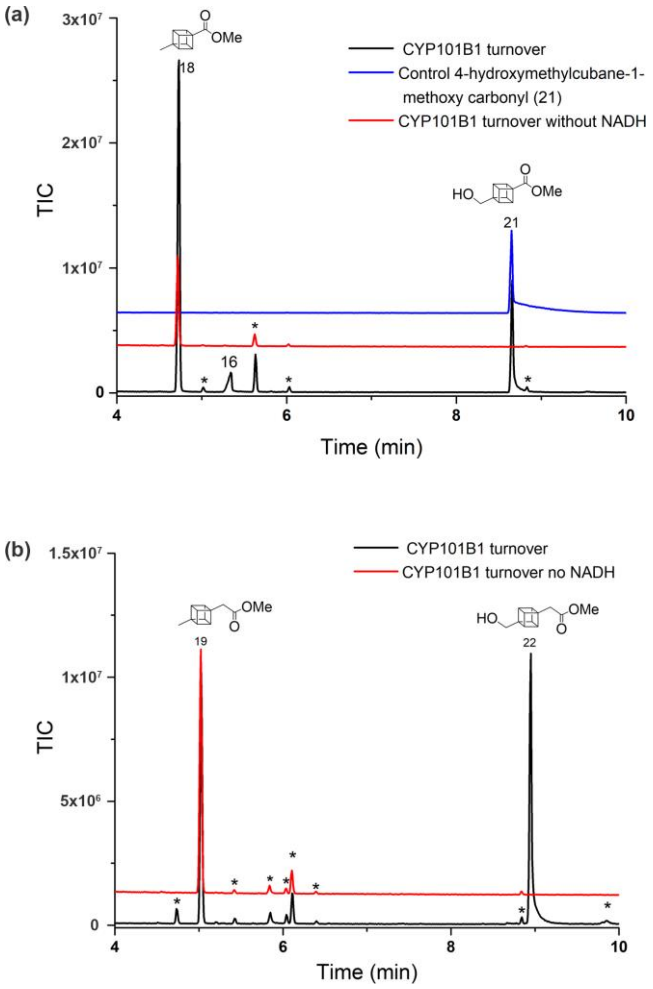

Figure 1 GC-MS analysis of the turnovers of (a) **18** and (b) **19** by CYP101B1. The turnovers are shown in black, a product control (**21**, see see Scheme 3b) is shown in blue, and a control turnover where no NADH was added is shown in red. Peaks labeled with asterisks represent impurities or products of non-enzymatic hydrolysis/transesterification (see SI for details).

Identification of the products of the CYP101B1-catalyzed oxidations of **18**–**20** was achieved by comparison with authentic samples of the plausible oxidized derivatives **21** and **23**–**25** (Scheme 3a). The cubylalkanols **21**–**24** correspond to site-selective hydroxylations of the methyl or ethyl C–H bonds of **18**–**20**. The homocubanol **25** could in principle be formed either by an enzyme-catalyzed oxidation of **18** following a cationic pathway, or by an acid-catalyzed rearrangement of the alcohol **21** post enzymatic hydroxylation of **18**. GC co-elution experiments with these product standards led to the assignment of the major products of the oxidations of **18** and **20** as cubylalkanols **21** and **23**, respectively (Scheme 3b).[12] The oxidation product of substrate **19** was assigned as cubylmethanol **22** by NMR and MS analysis followinga larger scale CYP101B1-catalyzed oxidation (*vide infra*). In the oxidation of **18**, no homocubanol **25** was detected, either by GC-MS or by GC based comparison with the authentic material. Likewise, no products with MS fragmentation patterns analogous to that of homocubanol **25** were observed in the CYP101B1-catalyzed oxidations of **19** or **20**.

Scheme 3 (a) Possible products and (b) assigned products of the CYP101B1-catalyzed oxidations of 18–20

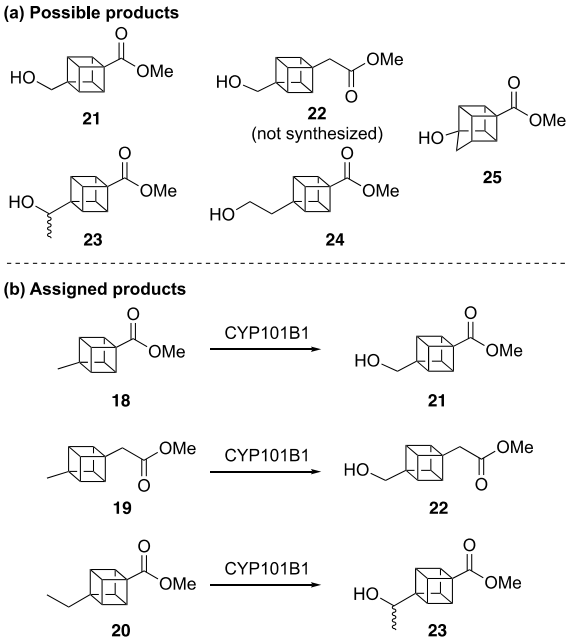

The CYP101B1-catalyzed oxidations of **18** and **19** were carried out on a larger scale using excess NADH in order to enable NMR analysis of the metabolite (Figures S2 and S4). GC-MS analysis of the extracted crude products showed that in each case, a single major product was present, identical to the one detected in the smaller scale experiments, and no detectable substrate remained. Minor products (<10%) were now also detectable, which were identified (using MS analysis and co-elution experiments) as originating from ester hydrolysis, transesterification, and further oxidation reactions involving the substrates and/or their oxidized products (Figures S2–S4).

The ^{1}H and ^{13}C NMR data of the crude extract from the oxidation of **18** agreed with the data of the authentic **21** product standard. The ^{1}H NMR spectrum showed a pair of characteristic signals in the range 3.9–4.2 ppm, each integrating to 3H, as expected for the intact 1,4-disubstituted cubane framework. A 2H singlet was present at 3.71 ppm, corresponding to the hydroxymethyl CH_2 group. If any rearranged products (namely ladderenes or bis-cyclobutenes,cf. Scheme 1) had been formed in these

oxidations, their *exo*-methylene protons would have been expected to resonate at approximately 4.5–4.7 ppm and their cyclobutene proton signals would have appeared in the range 5.8–6.6 ppm. No such signals were present in the ^{1}H NMR spectra of the crude extracts.^{1}H NMR analysis of crude **22** from **19** revealed analogous signals to those observed for **21** with the addition of a 2H singlet at 2.68 ppm for the methylene group adjacent to the ester moiety.

These larger scale experiments allowed the yield of **21** from the oxidation of **18** to be calculated.Calibration of the levels of substrate and product present after the oxidation revealed that CYP101B1 had converted 93 ± 10% of methylcubane **18** into cubylmethanol **21**. This is much higher than the yields reported previously for P450-catalyzed oxidations of parent methylcubane (<1%, Scheme 2). It further indicates that **21** itself is not a good substrate for CYP101B1.[13]

There was no evidence for hydroxylation of any of the cubane C–H bonds of **18**–**20** (Figure S4). To determine if CYP101B1 could indeed hydroxylate a cubane C–H bond, assays were performed on methyl cubane-1-carboxylate (**26**). This substrate proved capable of binding to the enzyme (20% HS) and initiating the catalytic cycle (as measured by NADH oxidation) but it furnished only trace amounts of an apparently monooxygenated metabolite (Figures S2, S3).

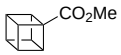

26

Chemical characterization of cubylmethyl radical rearrangements. The initially formed intermediates in the hydroxylations of substrates **18**–**20** would be expected to be the corresponding 4-substituted cubylmethyl radicals. Given the rapid skeletal rearrangement of the parent cubylmethyl radical **7** (k = 2.9 × 10^{10} s^{-1} at 25 °C, Scheme 1), it is very surprising to find no rearranged products in the oxidations of **18**–**20**.

In order to determine if the cubylmethyl radicals derived from the 4-substituted methylcubane derivatives **18**–**20** are somehow less reactive toward rearrangement than the parent cubylmethyl radical, the effects of the substituents on the first β-scission step were computed with quantum chemistry (Figure 2). Calculations with the high-accuracy CBS-QB3 method predicted small barriers ($\Delta G^{\ddagger}$) of 3.2 and 3.0 kcal/mol for the β-scission of the 4-methyl and 4-ester substituted cubylmethyl radicals **27** and **28**, respectively, equivalent to the calculated$\Delta G^{\ddagger}$ value for **7** itself (3.2 kcal/mol) and in very good agreement with the measured rate constant for **7** (calc. k = 2.8 × 10^{10} s^{-1}, expt. k = 2.9 × 10^{10} s^{-1}). These β-scissions are thermodynamically favored by >20 kcal/mol. The secondβ-scission (not shown), which is even faster, is downhill by a further 17 kcal/mol. All three radicals' rearrangements are therefore predicted to be extremely fast and effectively irreversible reactions. Carboxyl or carboxymethyl substituents at the 4-position are not anticipated to slow the rearrangement appreciably.

Radical	R	$\Delta G^{\ddagger}$	ΔG
7	H	3.2	–21.4
27	Me	3.2	–21.2
28	CO_2Me	3.0	–20.7

Figure 2. Barriers and energetics for the first β-scission step in the rearrangements of cubylmethyl radicals, calculated with CBS-QB3 (kcal/mol).

Several experiments were performed in an effort to chemically generate the cubylmethyl radical **28** (derived from substrate **18**) and study its reactivity (Scheme 4 and S6–S8). The expected rearranged products of **28**, after trapping by a hydrogen atom donor, are **29**–**31**. In two key experiments, shown in Scheme 4b, a Barton–McCombie deoxygenation of imidazole thiocarbamate ester **32** (Bu_3SnH/AIBN) and a Barton decarboxylation of *N*-hydroxypyridine-2-thione ester **34** ($h\nu$) were performed. Both reactions led to complex mixtures of products. Alkene(s) that may have been derived from a rearrangement of radical **28** comprised <5% of the products from both reactions observable by ^{1}HNMR spectroscopy. The major detectable products obtained from the reaction of **32** were carbamate **33** and the alcohol **21** (40% combined), both of which were likely formed through heterolytic pathways. In the attempted Barton decarboxylation reaction of **34**, a typical[14]thioether byproduct**35** was formed in 12% yield,suggesting that the cubylmethyl radical intermediate **28**wasindeed generated. By way of contrast, a Barton decarboxylation of the homologous acid **36** (Scheme 4c) gave ethylcubane derivative **20** in 91% yield, indicating that unlike the cubylmethyl radical, it is possible to efficiently introduce and trap a radical at a primary carbon β to the cube through chemical means.

Scheme 4. (a) Possible products formed from cubylmethyl radical 28 in the presence of a hydrogen atom donor; (b) Synthetic reactions designed to generate and trap cubylmethyl radical 28 and its rearrangement products; (c) Generation and trapping of a cubylethyl radical from 36

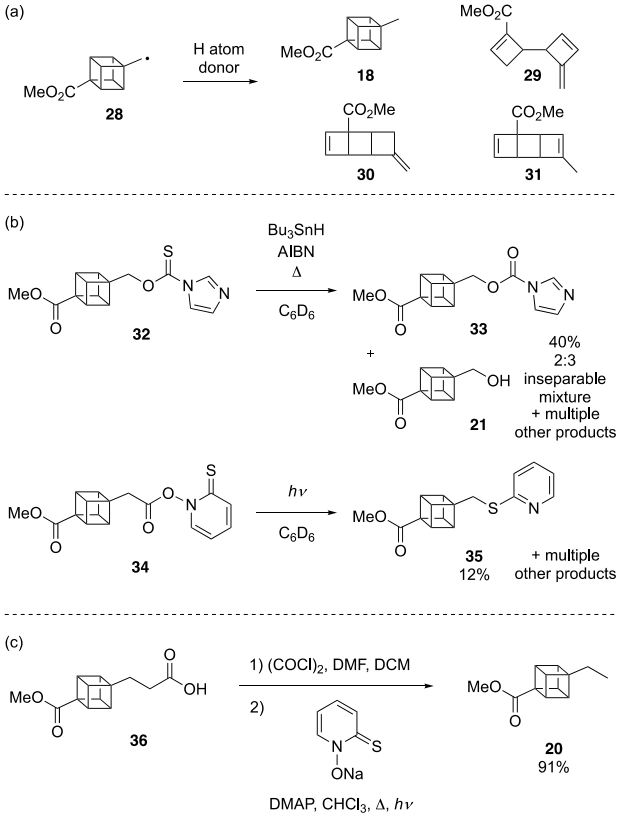

In general, the products of methylcubane rearrangements are highly susceptible to further reactions such as polymerization.8[a]This reactivity is likely to be compounded by the electron-withdrawing groups present in **29**–**31**. The absence of unraveled cubanes among the major products of the synthetic reactions depicted in Scheme 4b does not necessarily indicate that the cubylmethyl radical **28** was not formed; it more likely reflects the instability of the unraveled cubane toward further degradation. Of course, similar fragility would be expected for any unraveled cubane derivatives produced in the enzyme-catalyzed oxidations of **18**–**20**. However, if ladderene or bicyclobutenyl derivatives had indeed been formed in the enzyme-catalyzed processes but had quickly degraded, then significant losses of material would have been observed. In reality, the yields were high; e.g. **18** gave near quantitative conversion to cubylmethanol **21**. This sets the oxidations of methylcubanes **18**–**20** apart from all other previously studied P450-catalyzed methylcubane oxidations (Scheme 2). Their high yields mean that the formation of rearranged products can be ruled out with a level of confidence that was not possible in the previous (very low yielding) methylcubane oxidations.

Mechanistic implications. The use of radical clock probes tocharacterize enzymemechanisms and to quantify rebound rate constants involvesseveral caveats. These are briefly examined here as they relate to the mechanism of CYP101B1-catalyzed hydroxylation of **18**–**20**.

The first assumption is that the enzyme does indeed abstract a hydrogen atom from the substrate to generate a carbon-centered radical. The prevailing view of P450 catalysis is very much in favor of radical formation[21]and certainly,in the case of **18**–**20**, the absence of homocubanol products represents strong evidenceagainst a cationic pathway.Density functional theory (DFT) calculations (see the Supporting Information) using a heme–methylthiolate model of Cpd Isuggest that a P450 should have no special difficulty in abstracting a hydrogen atom from methylcubane to form a cubylmethyl radical.The energy profile for hydrogen atom abstraction by the model Cpd I is similar to those predicted by DFT for a range of other C–H bonds.[22–24]

A secondassumption is that the rate constant for theringopening of the radical clock probewithin the enzyme active site is the same as in bulk solution. Conceivably, an enzyme might impede the ringopening simply by physically constraining the radical within the active site. However, this appears unlikely for **18**–**20**, since CYP101B1 is able to specifically bind and efficiently oxidize larger substrates such as 2-adamantyl isobutyrate and cyclododecyl acetate, suggesting a sterically undemanding active site.[11f,g]Newcomb et al.[23c] explored similar ideas with a range of ultrafast probes; their findings with probes that underwent little molecular motion upon rearrangement, and with probes that underwent isotopically induced metabolic branching,led to the conclusionthat the rearrangements were not slowed in the enzyme.[15]Furthermore, calculationssuggest thatthe weak interaction of the radical with the (HO)Femoietyin the active sitedoes not have a significant effect on the rearrangement barrier for either cubylmethyl[16] or cyclopropylmethyl-type[17] radicals.

One furtherassumption normally made is that the rearrangement of the probe radical in the active site is irreversible.[18]For our cubylmethyl radicals, it seems very likely that the rearrangement is irreversible within the active site. DFT calculations (see SI) predict that the first β-scission of the cubylmethyl radicalin the presence of a model Cpd II is energetically downhill by 23 kcal/mol and the second β-scission (which is even faster than the first) is downhill by a further 17 kcal/mol. Returning to the non-rearranged radical faces a sizable kinetic barrier.

On this basis, it is concluded that the rearrangement rate constants for the radicals derived from **18**–**20** in the active site of CYP101B1 can be taken to beequivalent to the rate constant measured for the parent cubylmethyl radical**7** in solution, i.e. 3×10^{10} s^{-1}.The observed near-quantitative hydroxylation of **18**–**20** implies that the rebound of the cubylmethyl radicals must out-compete rearrangement by at least 1–2 orders of magnitude, from which it follows that the rebound rate constantsare$\geq 3 \times 10^{11}$–$10^{12}$$s^{-1}$.

Typical reported rate constants3 for radical rebound in P450-catalyzed hydroxylations are $2–3 \times 10^{10}$ s^{-1}. Therefore, substrates**18**–**20**arethe first examples of methylcubanes whose apparent rebound rates candefinitively be categorized as ultrafast.Several other ultrafast probes (e.g. methylphenylcyclopropyl type probes) have even faster apparent rebound rate constants,up to 1.2×10^{13} s^{-1}.3[g,10a,23d]The large variations observed for rebound rates, spanning a factor of 10^3, has led to much speculation about the mechanism and the nature of the radical "intermediate". Rebound rate constants of 3×10^{11}– $1.2 \times 10^{13}$$s^{-1}$imply radical lifetimes on the order of 0.08–3 picoseconds. These lifetimes, especially those in the sub-picosecond regime, are very short, almost bordering onthe lifetimes oftransition states (TSs), which are typically<60 femtoseconds.[19,20]As a group,the radicals derived from ultrafast P450 probe substratesseem to represent a special class of "intermediate" which, unlike normal P450 radical intermediates, do not survive long enough to equilibrate within the active site.

Previous explanations for unexpected ratios of rearranged to unrearranged products. Several theories have previously been advanced to account for the paradox of ultrafast rebound in P450-catalyzed oxidations.[21] The most widely accepted and versatile picture is the two-state model of reactivity developed by Shaik and coworkers.[22–24] In this picture, the reactive oxidant Cpd I exists in two almost equienergetic electronic states – a doublet (low spin, LS) and a quartet (high spin, HS). After hydrogen atom abstraction has taken place and the necessary reorientation of radical and Fe(OH) group with respect to each other has occurred, the energy profile for rebounddiffers depending on the spin state. On the HS potential energy surface a barrier of approximately 4 kcal/mol or more is found, but on the LS surface the barrier issmaller or even zero. This endows the HS intermediate with a longer lifetime than the LS intermediate, potentially making the HS intermediate the chief origin of any rearranged products and the LS intermediate the chief origin of unrearranged products. Apparent ultrafast rebound could be explained by this model if the flux through a barrierless LS rebound pathway is much greater than the flux through the HS pathway. Various factors have been proposed to influence the LS *vs* HS partitioning, including the donor ability of the radical, the geometry and strength of the bond to the proximal

ligand, and specific contributions from the protein environment.[1f,25]

DFT calculations (see SI) show that the two-state energy profile for methylcubane hydroxylation is fairly typical for a P450-catalyzed hydroxylation, with no unusual spin-state related effects. After the intermediate cubylmethyl radical has formed, its rebound onto FeOH to give the hydroxylated product has a small potential energy barrier of 3–4 kcal/mol in either spin state. The rearrangement of the cubylmethyl radical has a similar barrier, 3–4 kcal/mol, on both surfaces.Intinsically, therefore, the radical has comparable propensities toward rebound or rearrangement in either spin state.The exact spin-state preference for CYP101B1 cannot easily be determined. Whilst a mechanism in which one spin state dominates cannot be ruled out, there is no obvious reason why this should be assumed to be the case. *Could an alternative picture equally explain the apparent ultrafast rebound?*

Groves3[g,h]has drawn attention to the importance of cage effects in determining the ratios of rearranged to unrearranged products obtained from radical clock probes. Apart from the rebound orrearrangement of the incipient caged radical [R•…(HO)Fe], an alternative pathway is cage escape, where R• and (HO)Fe become separated by a solvent molecule or active site side chain.The escaped R• eventually rearranges before recombining with (HO)Fe. For radicals that rearrangerelatively slowly, greater-than-expected ratios of rearranged to unrearranged products can be produced if cage escape competes with rebound. This behavior has been observed, for example, for a series of bicyclic cyclopropylcarbinyl-type probes.3[i] The hydroxylations of **18**–**20** display the exact opposite effect (not as much rearrangementas expected), suggesting that in these reactions the reverse situation is in play: namely, R• is kept close to Fe(OH) by complementary enzyme–substrate binding. Given that any slowing of the rearrangement due to steric constraints or due to the R•…(HO)Fe interaction in the active site is not supported by our evidence (discussed above), it seems likely that the key to the lack of rearrangement is a specific enzyme–substrate binding interaction, presumably involving the carbonyl functionality of **18**–**20** and one or more hydrogen bond donors in CYP101B1.

Dynamical coupling of hydrogen abstraction and radical rebound. We propose that a more complete picture of P450 catalysis can be gained by considering not only two-state reactivity but alsothe way in which the enzyme controls the reaction trajectory. Some simple considerations about enzyme–substrate binding lead to the prediction that the C–H abstraction and rebound phases of the hydroxylation can be brought close together in time to form a process that is“dynamically concerted”,or nearly so.[26]

A reaction consisting of two bond-forming/breaking processes is defined as dynamically concerted if the time gap between the first and second bond forming/breaking events is less than 60 fs (this being the lifetime for a transition state with a zero energy barrier).[26] If the time gap is longer than 60 fs, the reaction is defined as dynamically stepwise. As aparadigm for understanding reactivity, this type of dynamical effecthas been rapidly gaining prominence,with relevance to both small-molecule transformations and enzyme-catalyzed processes.[20,27]

To illustrate how dynamical effects may lead to ultrafast P450-catalyzed hydroxylation, Figure 3a shows the potential energy surface for methylcubane oxidation by a heme–methylthiolate model of Cpd I, calculated with DFT.[16] This surface represents a reaction occurring in a solvent continuum in the HS state. The medium has a polarity similar to that of the interior of an enzyme, but has no explicitly modeled solvent molecules or functional groups around the substrate and Fe complex. The energy surface is projected onto two coordinates representing the C–H distance and the COH angle. Together these two coordinates differentiate the hydrogen abstraction and rebound processes, as shown by the arrows in Figure 3a. Starting from the hydrogen abstraction TS at the lower left of the diagram, the minimum energy path (arrow 1) leads downhill onto a broad plain where the radical intermediate resides. Before rebound can occur, the radical and OH group must reorient so that the singly occupied orbital of the radical can overlap with oxygen to form the C–O bond (arrow 2). A large change of about 60° in the COH angle occurs during this process. Movement along the reorientational coordinate leads to a small energy barrier at the rebound TSand then a steep downhill pathway to the alcohol product (arrow 3).

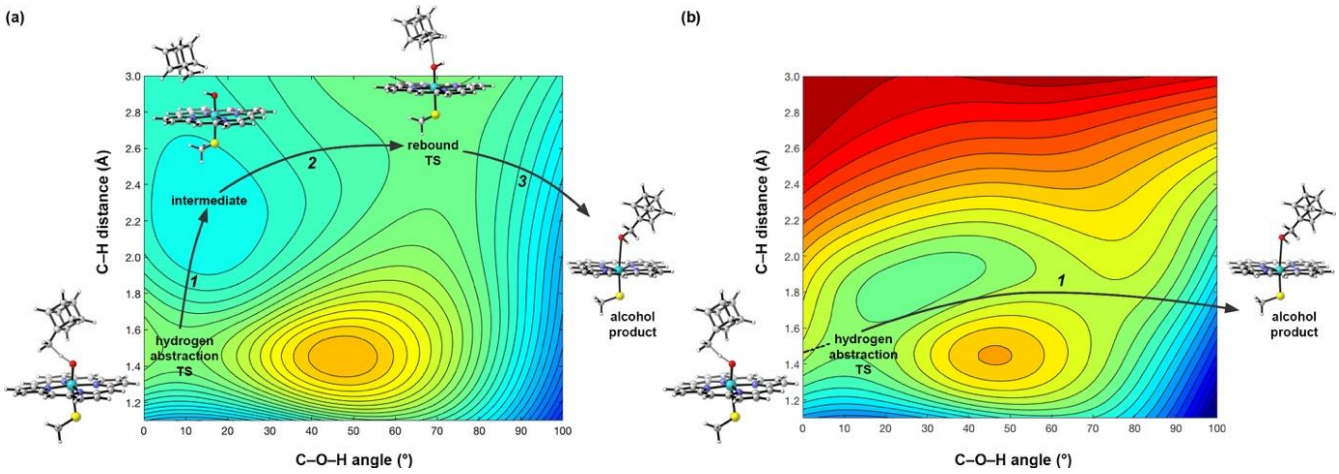

Figure 3. (a) Potential energy surface (high spin) for the hydroxylation of methylcubane by a model Cpd I, calculated with B3LYP-D3(BJ)/6-31G(d)-LANL2DZ in implicit (CPCM) diethyl ether. (b) Hypothetical effect of merging the hydrogen atom abstraction and

rebound steps into a dynamically concerted process as a result of complementary enzyme–substrate binding. The surface in (b) was generated by raising the energies of the points in the upper portion of (a) to simulate holding R• in proximity to Fe(OH).

An important aspect of this energy surface is that after the hydrogen atom abstraction has taken place, some time will elapse while the energy of the intermediate becomes redistributed into the appropriate nuclear modes to enable the radical and Fe(OH) to align appropriately for C–O bond formation. The most important modes involve the repositioning of R• with respect to Fe(OH) and the torsion around the Fe–OH bond. During this energy redistribution phase, the radical would roam easily around the shallow energy well. This period of time is when the radical is most likely to undergo side reactions such as skeletal rearrangement.

In general, reactions occurring on energy surfaces with shallow intermediates following a large initial energy barrier (of which the reaction in Figure 3a is an example) are influenced by non-statistical dynamics. Dynamically concerted pathways enable a reaction to avoid competing fates for the intermediate since the bond forming/breaking events are brought close together in time, within approximately the period of a molecular vibration.

A dynamically concerted (or nearly so) reactionwithin the confines of the CYP101B1 active site provides a way to explain the apparent ultrafast rebound of**18**–**20** even without invoking any preference for LS *vs* HS pathways. In the model reaction (Figure 3a), once the hydrogen atom abstraction TS has been passed, continued motion along the C–H abstraction coordinate has a negligible potential energy barrier. However, within an enzyme this type of motion would be restricted, either through general steric confinement or through specific enzyme–substrate interactions in the active site. Under these circumstances, the flat region at the top left of the energy surface is replaced by a wall, preventing R• from moving away from Fe(OH). This scenario is represented schematically in Figure 3b, where the energies of points in the upper portion of the diagram from Figure 3a have been raised to simulate the effect of these active site constraints. The reactive trajectories on this surface are different from those in the model reaction: they will be concentrated in a channel where R• remains in close proximity to Fe(OH). The hydrogen atom abstraction and rebound steps are now more tightly coupled, shortening the lifetime of the intermediate [R•…(HO)Fe] (arrow 1 in Figure 3b). This minimizesthe opportunity for the radical to undergo side reactions (rearrangement in this case). The apparent ultrashort radical lifetime is no longer paradoxical, since the "cubylmethyl radical" formed during the reaction is chemically different from the one formed in the solution-phase kinetic studies in which the rearrangement rate was measured; it does not have the opportunity to equilibrate.[28]

The energy surfaces in Figure 3 depict the HS state. We utilized the HS state for these calculations because HS is the state most likely to follow a stepwise mechanism in the conventional two-state reactivity paradigm.[16] HS is therefore the state in which dynamical effects would need to be strongest if they were to be responsible for bringing about an apparently concerted hydroxylation. However, the same general principles about the reaction trajectory apply more or less equally to both the HS and the LS states. Our calculations show that the two states have similar general energetic features in methylcubane oxidation. Even though the LS mechanism of a P450 hydroxylation is generally regarded as effectively concerted in the sense that C–O bond formation often has a negligible energy barrier, it still has the same reorientation phase in between hydrogen abstraction and rebound and is therefore still capable of experiencing a time delay between those two processes, during which rearrangement could occur.[29] This idea is supported by recent molecular dynamics simulations[30] on the oxidation of propane, which showed that, out of 101 trajectories of the model LS Cpd II run for 3.6 ps at 300 K in the gas phase, 46 trajectories gave the alcohol while one trajectory led to the [R•…(HO)Fe] complex (the other trajectories reverted to reactants or underwent desaturation). A complete lack of side-reactivity would likely require both the LS and HS reactions to feature dynamically coupled hydrogen abstraction and rebound.

How might the enzyme enact dynamically coupled hydrogen abstraction and rebound? There are likely many contributing factors, but two seem especially important: firstly, controlling the redistribution of the excess energy into the relevant reorientational modes after hydrogen atom abstraction (i.e., motion of R• relative to Fe(OH) or torsion around the Fe–OH bond), and secondly, setting up a specific approach trajectory towards the hydrogen abstraction transition state. As is evident in Figure 3b, trajectories that approach the hydrogen atom abstraction transition state from a more oblique angle (e.g. dashed line) are most likely to proceed entirely downhill thereafter, bypassing the intermediate. This would entail passing through transition structures that differ from the ideal linear C–H–O alignment.[31]

The high level of regioselectivity observed in the oxidations of **18**–**20** highlights the importance of the carbonyl functionality engaging in specific enzyme–substrate interactions to control both the reaction mechanism and the site selectivity. The oxidations of methylcubane by other P450s (Scheme 2) are much less selective but they still produce some cubylmethanol (**2**), potentially also by a dynamically coupled mechanism. The formation of rearranged products cannot be ruled out in those examples due to low recovery of materials but it appears likely that in such low-yielding and unselective reactions, stepwise pathways would also be expected, leading to some rearrangement.

In general, a dynamics-centric picture of P450 reactivity predicts that the species formed by hydrogen atom abstraction from the substrate may appear to behave as either a typical intermediate or more similar to a transition state, depending on how tightly the enzyme controls the reactive trajectory.[27] The observed lifetime of the "intermediate" would be the average of the lifetimes of all trajectories which individually could range from stepwise toward dynamically concerted and thus explain situations where mixtures of rearranged and unrearranged products are formed from ultrafast probe substrates.[32] The idea of dynamically bypassing a radical intermediate in P450-catalyzed hydroxylations was previously noted by Shaik*et al.*, who suggested that it would represent an alternative to the two-state reactivity paradigm.[25] Functionally, a reaction in which both dynamically concerted and dynamically stepwise trajectories are possible would be equivalent to a reaction in which a discrete intermediate favors different products on the LS and HS surfaces. While two-state reactivity and dynamics can each independently account for ultrafast rebound, it seems more likely that the dynamical

concepts are a complement to, rather than a replacement for, the two-state reactivity paradigm. Both are important.

In addition to explaining the variation observed in rebound rates with differing cyclopropyl radical clocks and why ultrafast probes such as methylphenylcyclopropanes[33] and their contrained analogues[23c]appear to undergo less rearrangement that expected, dynamical pictures can also be proposed to explain a range of other aspects of cytochrome P450 reactivity. For example, different degrees of dynamical concertedness could explain why the mechanisms of oxidations catalyzed by a certain P450 vary depending on the nature of the enzyme–substrate pairing. In the oxidations of cyclopropyl-containing fatty acids **37**(Scheme 5a) by P450BM3, long-chain (C_{16}) substrates underwent ring opening solely by a radical mechanism whereas shorter-chain (C_{12}) substrates (which were a poorer fit in the active site) reacted through both radical and cationic pathways.[34] For the C_{12} substrates, the cation-derived products are believed to result from electron transfer to the heme Fe(OH) complex from the intermediate radical. A change in preference from tightly coupled hydrogen abstraction + rebound for C_{16} substrates to less tightly coupled pathways for C_{12} substrates would explain the formation of both cation- and radical-derived products from the C_{12} substrates.

Scheme 5.Some aspects of P450 reactivity that may be explained by dynamical effects. (a)Substrate-dependentpathway variations involving radical *vs* cation formation; (b) variations in rebound rates in the oxidations of diastereomeric substrates proceeding via a common radical.

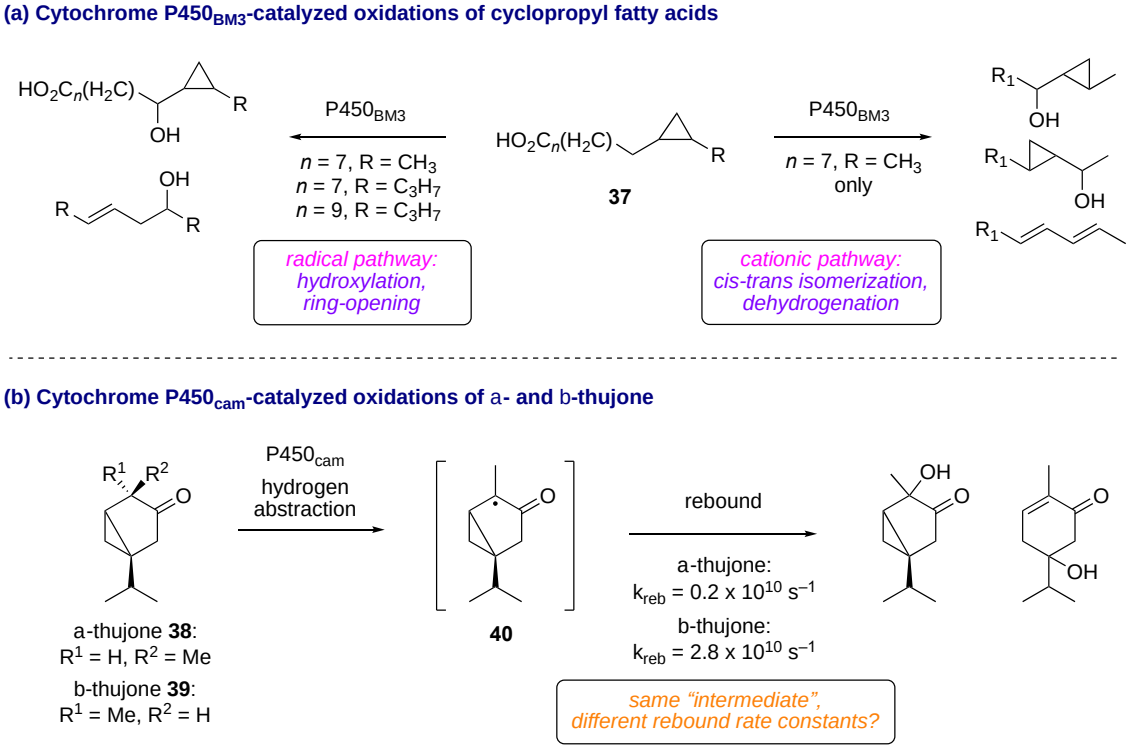

Related dynamical ideas could explain the unexpected variations in rebound rates observed for certain probe substrates whose structures differ in subtle stereochemical ways, e.g. the oxidations of α-thujone (**38**) and β-thujone (**39**) by $P450_{cam}$ (Scheme 5b).[35] These oxidations ostensibly proceed via the same radical intermediate (**40**), yet their rebound rates differ by an order of magnitude. Differences in the geometry of the P450–substrate interaction at the outset of the hydrogen abstraction would be expected to define different reactive trajectories characterized by distinct radical lifetimes, thereby accounting for the apparent difference in rebound rates. Two-state reactivity is less able to explain this behavior.

Conversely, in other enzyme–substrate pairs, a tightly controlled stepwise trajectory could be strategically used by Nature to favor the formation of a discrete radical intermediate. This would be a way to divert the radical towardalternative fates prior to (or instead of) rebound. An example would be P450-catalyzed dehydrogenation reactions, which are thought to involve single-electron oxidation or hydrogen atom abstraction of the initially formed radical.[34,36] In this case, steering the course of the reaction through a stepwise pathway would ensure a longer lifetime for the intermediate, giving it the time to transfer an electron or hydrogen atom to the heme Fe–OH group. These examples illustrate just a few of the possible impacts of dynamical control over P450 reactivity. There is a great deal of scope for the generality of these dynamical effects to be tested computationally by means of molecular dynamics trajectory calculations and experimentally by careful design and selection of probe/P450 pairs.

In sum, substrates bound with high specificity and held in an optimal orientation relative to Cpd I could lead to a hydroxylationmechanism that approaches dynamical concertedness. Non-optimally bound substrates may instead follow a trajectory that results in a slower rebound leading to a

stepwise reaction with a longer-lived radical intermediate.Multiple orientations of the substrate could lead to a mixture of both of these pathways, leading to experimental results characteristic of either or both concerted and non-concerted reactions. Irrespective of the specific assumptions on which our analysis of the CYP101B1/methylcubane system is based, the relevance of dynamical conceptstoenzyme catalysis is expected to be wide ranging.

CONCLUSIONS

We have demonstrated that a cytochrome P450 efficiently and selectively hydroxylates the methyl group of methylcubane derivatives designed to bind specifically to the active site of the enzyme with the methyl group proximal to the reactive iron-oxo moiety. Hydroxylation solely at the methyl group of a methylcubane is very difficult to achieve using chemical methodologies, due to the fast skeletal rearrangements of the cubylmethyl radical (or cation) intermediate, yet the CYP101B1 enzyme from *N. aromaticivorans* delivers cubylmethanols in high yield without any evidence for rearrangement of the cubane core. These unexpectedly efficient hydroxylations are proposed to reflect a mechanistic paradigm in which the enzyme controls the degree of dynamical concertedness of the reaction. Bringing the C–H abstraction and C–O bond formation steps close together in time effectively bypasses the cubylmethyl radical intermediate, such that the radical loses the opportunity to undergo otherwise fast side reactions. This type of dynamical picture of P450 reactivity represents a second possible explanation for apparent ultrafast rebound rates, alongside the well tested two-state reactivity paradigm. Both models may well be equally important. A variety of examples of P450 catalysis are presented that potentially can be explained in dynamical terms, which could in future be probed by molecular dynamics trajectory calculations. Overall, this work adds a further nuance to the complex dynamical picture of P450 catalysis, which more broadly involves coordinated motions of enzyme and substrate occurring during substrate binding, oxidation, and product release.

ASSOCIATED CONTENT

Supporting Information

Complete experimental details, GC-MS, NMR, and MS data, and computational methods and data.The Supporting Information is available free of charge on the ACS Publications website.

AUTHOR INFORMATION

Corresponding Author

* stephen.bell@adelaide.edu.au;c.williams3@uq.edu.au; e.krenske@uq.edu.au; j.devoss@uq.edu.au.

Present Address

^Department of Pharmaceutical Technology, University of Dhaka, Dhaka, Bangladesh.

ORCID

Md. Raihan Sarkar: 0000-0003-4807-5071
Sevan Houston:0000-0002-9309-7037
Paul Savage:0000-0001-7805-8630
Craig Williams: 0000-0002-3834-7398
Elizabeth Krenske: 0000-0003-1911-0501
Stephen Bell: 0000-0002-7457-9727
James De Voss: 0000-0002-2659-5140

Author Contributions

§These authors contributed equally.

Notes

CSIRO (G. P. S.) and UQ (C. M. W.) have a formal relationship with Boron Molecular Pty Ltd who supply cubane intermediates.

ACKNOWLEDGMENT

We thank the University of Adelaide and the University of Queensland (UQ) for financial support. Md.R.S. thanks the University of Adelaide for an International PhD scholarship. S.D.H. gratefully acknowledges the Northcote Trust and Britain-Australia Society for their award of the Northcote Graduate Scholarship. The financial support of the Australian Research Council (FT140100355 to S.G.B, FT110100851 to C.M.W., DP180103047 to E.H.K.) is gratefully acknowledged. Computer resources were provided by the National Facility of the Australian National Computational Infrastructure through the National Merit Allocation Scheme and by the University of Queensland Research Computing Centre. Prof. P. V. Bernhardt and Mr. T. Vanden Berg are thanked for collecting and solving, respectively, the X-ray crystallographic structure of 1,4-diiodocubane.

REFERENCES

1.(a) Ahalawat, N.; Mondal, J.Mapping the substrate recognition pathway in cytochrome P450.*J. Am. Chem. Soc.***2018**, *140*, 17743. (b) Chen, K.; Zhang, S.-Q.; Brandenberg, O. F.; Hong, X.; Arnold, F. H.Alternate heme ligation steers activity and selectivity in engineered cytochrome P450-catalyzed carbene-transfer reactions.*J. Am. Chem. Soc.***2018**, *140*, 16402. (c) Guengerich, F. P. Mechanisms of cytochrome P450-catalyzed oxidations.*ACS Catal.***2018**, *8*, 10964. (d) Lewis, R. D.; Garcia-Borràs, M.; Chalkley, M. J.; Buller, A. R.; Houk, K. N.; Kan, S. B. J.; Arnold, F. H.Catalytic iron-carbene intermediate revealed in a cytochrome c carbene transferase.*Proc. Natl. Acad. Sci U. S. A.***2018**, *115*, 7308. (e) Zaragoza, J. P. T.; Yosca, T. H.; Siegler, M. A.; Moënne-Loccoz, P.; Green, M. T.; Goldberg, D. P. Direct observation of oxygen rebound with an iron-hydroxide complex.*J. Am. Chem. Soc.***2017**, *139*, 13640. (f) Ramanan, R.; Dubey, K. D.; Wang, B.; Mandal, D.; Shaik, S. Emergence of function in P450-proteins: A combined quantum mechanical/molecular mechanical and molecular dynamics study of the reactive species in the H_2O_2-dependent cytochrome $P450_{SP\alpha}$ and its regio- and enantioselective hydroxylation of fatty acids. *J. Am. Chem. Soc.***2016**, *138*, 6786.

2. See, for example: (a) Alkhalaf, L. M.; Barry, S. M.; Rea, D.; Gallo, A.; Griffiths, D.; Lewandowski, J. R.; Fulop, V.; Challis, G. L. Binding of distinct substrate conformations enables hydroxylation of remote sites in thaxtomin D by cytochrome P450 TxtC.*J. Am. Chem. Soc.***2019**, *141*, 216. (b) Tsutsumi, H.; Katsuyama, Y.; Izumikawa, M.; Takagi, M.; Fujie, M.; Satoh, N.; Shin-ya, K.; Ohnishi, Y. Unprecedented cyclization catalyzed by a cytochrome P450 in benzastatin biosynthesis.*J. Am. Chem. Soc.***2018**, *140*, 6631. (c) Nagel, R.; Peters, R. J. Diverging mechanisms: cytochrome-P450-catalyzed demethylation and γ-lactone formation in bacterial gibberellin biosynthesis.*Angew. Chem. Int. Ed.***2018**, *57*, 6082. (d) Dang, T.-T. T.; Franke, J.; Tatsis, E.; O'Connor, S. E. Dual catalytic activity of a cytochrome P450 controls bifurcation at a metabolic branch point of alkaloid biosynthesis in *Rauwolfia serpentina*.*Angew. Chem. Int. Ed.***2017**, *56*, 9440. (e)) Grant, J. L.; Mitchell, M. E.; Makris, T. M. Catalytic strategy for carbon−carbon bond scission by the cytochrome P450 OleT. *Proc. Natl. Acad. Sci. U. S. A.***2016**, *113*, 10049.

3. (a) Ortiz de Montellano, P. R. Substrate Oxidation by Cytochrome P450 Enzymes.In *Cytochrome P450: Structure, Mechanism, and Biochemistry*, 4th edition.; Ortiz de Montellano, P. R., Eds.; Springer: Switzerland, 2015, Vol. 1, Ch 4. (b) Ortiz de Montellano, P. R. Hydrocarbon hydroxylation by cytochrome P450 enzymes.*Chem. Rev.***2010**, *110*, 932. (c) Denisov, I. G.; Makris, T. M.; Sligar, S. G.; Schlichting, I. Structure and chemistry of cytochrome P450.*Chem. Rev.***2005**, *105*, 2253. (d) Poulos, T. L. Heme enzyme structure and function.*Chem. Rev.***2014**, *114*, 3919. (e) Rittle, J.; Green, M. T. Cytochrome P450 compound I: capture, characterization, and C-H bond activation kinetics.*Science***2010**, *330*, 933. (f) Groves, J. T.; McClusky, G. A. Aliphatic hydroxylation via oxygen rebound. Oxygen transfer catalyzed by iron.*J. Am. Chem. Soc.***1976**, *98*, 859. (g) Huang, X.; Groves, J. T. Beyond ferryl-mediated hydroxylation: 40 years of the rebound mechanism and C–H activation.*J. Biol. Inorg. Chem.***2017**, *22*, 185. (h) Cooper, H. L. R.; Groves, J. T. Molecular probes of the mechanism of cytochrome P450. Oxygen traps a substrate radical intermediate. *Arch. Biochem. Biophys.***2011**, *507*, 111. (i) Austin, R. N.; Luddy, K.; Erickson, K.; Pender-Cudlip, M.; Bertrand, E.; Deng, D.; Buzdygon, R. S.; van Beilen, J. B.; Groves, J. T. Cage escape competes with geminate recombination during alkane hydroxylation by the diiron oxygenase AlkB. *Angew. Chem. Int. Ed.***2008**, *47*, 5232.

4. Auclair, K.; Hu, Z.; Little, D. M.; Ortiz de Montellano, P. R.; Groves, J. T. Revisiting the mechanism of P450 enzymes with the radical clocks norcarane and spiro[2,5]octane.*J. Am. Chem. Soc.***2002**, *124*, 6020.

5. (a) Biegasiewicz, K. F.; Griffiths, J. R.; Savage, G. P.; Tsanaktsidis, J.; Priefer, R. Cubane: 50 years later.*Chem. Rev.***2015**, *115*, 6719. (b) Doedens, R. J.; Eaton, P. E.; Fleischer, E. B. The bent bonds of cubane.*Eur. J. Org. Chem.***2017**, 2627. (c) Annese, C.; D'Accolti, L.; Fusco, C.; Gandolfi, R.; Eaton, P. E.; Curci, R. Oxyfunctionalization of non-natural targets by dioxiranes. 6. On the selective hydroxylation of cubane. *Org. Lett.***2009**, *11*, 3574. (d) Fokin, A. A.; Lauenstein, O.; Gunchenko, P. A.; Schreiner, P. R. Halogenation of cubane under phase-transfer conditions: single and double C–H-bond substitution with conservation of the cage structure. *J. Am. Chem. Soc.***2001**, *123*, 1842.

6. (a) Eaton, P. E. Cubanes: starting materials for the chemistry of the 1990s and the new century.*Angew. Chem. Int. Ed.* **1992**, *31*, 1421. (b) Wlochal, J.; Davies, R. D. M.; Burton, J. Cubanes in medicinal chemistry: synthesis of functionalized building blocks.*Org. Lett.***2014**, *16*, 4094. (c) Chalmers, B. A.; Xing, H.; Houston, S.; Clark, C.; Ghassabian, S.; Kuo, A.; Cao, B.; Reitsma, A.; Murray, C.-E. P.; Stok, J. E.; Boyle, G. M.; Pierce, C. J.; Littler, S. W.; Winkler, D. A.; Bernhardt, P. V.; Pasay, C.; De Voss, J. J.; McCarthy, J.; Parsons, P. G.; Walter, G. H.; Smith, M. T.; Cooper, H. M.; Nilsson, S. K.; Tsanaktsidis, J.; Savage, G. P.; Williams, C. M. Validating Eaton's hypothesis: cubane as a benzene bioisostere.*Angew. Chem. Int. Ed.***2016**, *55*, 3580. (d) Wlochal, J.; Davies, R. D. M.; Burton, J. Synthesis of novel amino acids containing cubane. *Synlett***2016**, *27*, 919.(e) Auberson, Y. P.; Brocklehurst, C.; Furegati, M.; Fessard, T. C.; Koch, G.; Decker, A.; La Vecchia, L.; Briard, E. Improving nonspecific binding and solubility: bicycloalkyl groups and cubanes as *para*-phenyl bioisosteres.*ChemMedChem***2017**, *12*, 590.(f) Xing, H.; Houston, S. D.; Chen, X.; Ghassabian, S.; Fahrenhorst-Jones, T.; Kuo, A.; Murray, C.-E. P.; Conn, K.-A.; Jaeschke, K. N.; Jin, D.-Y.; Pasay, C.; Bernhardt, P. V.; Burns, J. M.; Tsanaktsidis, J.; Savage, G. P.; Boyle, G. M.; De Voss, J. J.; McCarthy, J.; Walter, G. H.; Burne, T. H. J.; Smith, M. T.; Tie, J.-K.; Williams, C. M. Cyclooctatetraene: a bioactive cubane paradigm complement.*Chem. Eur. J.***2019**, *25*, 2729. (g) Houston, S. D.; Chalmers, B. A.; Savage, G. P.; Williams, C. M. Enantioselective synthesis of (*R*)-2-cubylglycine including unprecedented rhodium mediated C–H insertion of cubane.*Org. Biomol. Chem.***2019**, *17*, 1067. (h) Reekie, T. A.; Williams, C. M.; Rendina, L. M.; Kassiou, M. Cubanes in medicinal chemistry.*J. Med. Chem.***2019**, *62*, 1078. (i) Mykhailiuk, P. K. Saturated bioisosteres of benzene: where to go next? *Org. Biomol. Chem.***2019**, *17*, 2839. (j) Houston, S. D.; Fahrenhorst-Jones, T.; Xing, H.; Chalmers, B. A.; Sykes, M. L.; Stok, J. E.; Farfan Soto, C.; Burns, J. M.; Bernhardt, P. V.; De Voss, J. J.; Boyle, G. M.; Smith, M. T.; Tsanakstidis, J.; Savage, G. P.; Avery, V. M.; Williams, C. M. The cubane paradigm in bioactive molecule discovery: further scope, limitations and the cyclooctatetraene complement. *Org. Biomol. Chem.***2019**, *17*, 6790. (k) Xing, H.; Houston, S. D.; Chen, X.; Jin, D.-Y.; Savage, G. P.; Tie, J.-K.; Williams, C. M. Determining the necessity of phenyl ring π-character in warfarin. *Bioorg. Med. Chem. Lett.***2019**, *29*, 1954.

7. Zhang, Q. L.; Chen, B. Z. DFT studies on the cascade rearrangement reactions of the cubylcarbinyl radical.*J. Phys. Org. Chem.***2011**, *24*, 147.

8. (a) Eaton, P. E.; Yip, Y. C. The preparation and fate of cubylcarbinyl radicals.*J. Am. Chem. Soc.***1991**, *113*, 7692. (b) Choi, S. Y.; Eaton, P. E.; Newcomb, M.; Yip, Y. C. Picosecond radical kinetics. Bond cleavage of the cubylcarbinyl radical.*J. Am. Chem. Soc.***1992**, *114*, 6326. (c) Della, E. W.; Head, N. J.; Mallon, P.; Walton, J. C. Homolytic reactions of cubanes. Generation and characterization of cubyl and cubylcarbinyl radicals. *J. Am. Chem. Soc.***1992**, *114*, 10730. (d) Newcomb, M. Competition methods and scales for alkyl radical reaction kinetics.*Tetrahedron***1993**, *49*, 1151.

9. Choi, S. Y.; Eaton, P. E.; Hollenberg, P. F.; Liu, K. E.; Lippard, S. J.; Newcomb, M.; Putt, D. A.; Upadhyaya, S. P.; Xiong, Y. S. Regiochemical variations in reactions of methylcubane with *tert*-butoxyl radicals, cytochrome P-450 enzymes, and a methane monooxygenase system.*J. Am. Chem. Soc.***1996**, *118*, 6547.

10. (a) Newcomb, M.; Shen, R.; Choi, S. Y.; Toy, P. H.; Hollenberg, P. F.; Vaz, A. D. N.; Coon, M. J. Cytochrome P450-catalyzed hydroxylation of mechanistic probes that distinguish between radicals and cations. Evidence for cationic but not for

radical intermediates.*J. Am. Chem. Soc.***2000**, *122*, 2677. (b) Jin, Y.; Lipscomb, J. D. Probing the mechanism of C–H activation: oxidation of methylcubane by soluble methane monooxygenase from *Methylosinus trichosporium* OB3b. *Biochemistry***1999**, *38*, 6178.

11. (a) Bell, S. G.; Wong, L. L. P450 enzymes from the bacterium *Novosphingobium aromaticivorans*.*Biochem. Biophys. Res. Commun.***2007**, *360*, 666. (b) Bell, S. G.; Dale, A.; Rees, N. H.; Wong, L. L. A cytochrome P450 class I electron transfer system from *Novosphingobium aromaticivorans*.*Appl. Microbiol. Biotechnol.***2010**, *86*, 163. (c) Yang, W.; Bell, S. G.; Wang, H.; Zhou, W.; Hoskins, N.; Dale, A.; Bartlam, M.; Wong, L. L.; Rao, Z. Molecular characterization of a class I P450 electron transfer system from *Novosphingobium aromaticivorans* DSM12444.*J. Biol. Chem.***2010**, *285*, 27372. (d) Hall, E. A.; Bell, S. G. The efficient and selective biocatalytic oxidation of norisoprenoid and aromatic substrates by CYP101B1 from *Novosphingobium aromaticivorans* DSM12444. *RSC Adv.***2015**, *5*, 5762. (e) Hall, E. A.; Sarkar, M. R.; Lee, J. H. Z.; Munday S. D.; Bell, S. G. Improving the monooxygenase activity and the regio- and stereoselectivity of terpenoid hydroxylation using ester directing groups.*ACS Catal.***2016**, *6*, 6306. (f) Sarkar, M. R.; Hall, E. A.; Dasgupta, S.; Bell, S. G. The use of directing groups enables the selective and efficient biocatalytic oxidation of unactivated adamantyl C-H bonds.*ChemistrySelect***2016**, *1*, 6700. (g) Sarkar, M. R.; Dasgupta, S.; Pyke, S. M.; Bell, S. G. Selective biocatalytic hydroxylation of unactivated methylene C–H bonds in cyclic alkyl substrates. *Chem. Commun.***2019**, *55*, 5029.

12. The MS fragmentation patterns of **21** and **23** indicated that the cubane skeleton remained intact (Figure S3).

13. Newcomb et al. previously reported a similar finding, showing that cubylmethanol **2** was not a substrate for CYP2B4.10[a]

14. Newcomb, M.; Kaplan, J. Rate constants and Arrhenius function for scavenging of octyl radical by an N-hydroxypyridine-2-thione ester. *Tetrahedron Lett.***1987**, *28*, 1615.

15. The structures of the cubylmethyl radical **7** and its ring-opened products **8** and **9**, computed as part of the CBS-QB3 calculations (shown below), suggest that these twoβ-scissionsproduce only a relatively small change in the volume of space occupied by the radical.

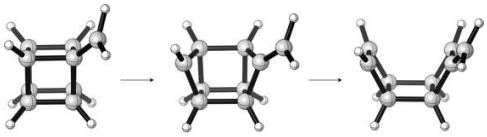

7 **8** **9**

16. See the Supporting Information for details.

17. The possibility that the rate of rearrangement is affected by the weak interaction of R• with (HO)Fe has been considered by several groups. Calculations on rearrangements of cyclopropylmethyl type radicals suggested that the R•…(HO)Fe interaction did not have a significant effect on the rearrangement barrier (at least in model systems lacking the steric contraints of an enzyme active site). See: (a) Kumar, D.; de Visser, S. P.; Sharma, P. K.; Cohen, S.; Shaik, S. Radical clock substrates, their C–H hydroxylation mechanism by cytochrome P450, and other reactivity patterns: what does theory reveal about the clocks' behavior?*J. Am. Chem. Soc.***2004**, *126*, 1907. (b) Jäger, C.; Hennemann, M.; Clark, T. The effect of a complexed lithium cation on a norcarane-based radical clock.*Chem. Eur. J.***2009**, *15*, 2425.

18. Frey, P. A. Radicals in enzymatic reactions. *Curr. Opin. Chem. Biol.***1997**, *1*, 347.

19. Schramm, V. Transition states and transition state analogue interactions with enzymes. *Acc. Chem. Res.***2015**, *48*, 1032.

20. Patel, A.; Chen, Z.; Yang, Z.; Gutiérrez, O.; Liu, H.-w.; Houk, K. N.; Singleton, D. A. Dynamically complex [6+4] and [4+2] cycloadditions in the biosynthesis of spinosyn A. *J. Am. Chem. Soc.***2016**, *138*, 3631.

21. An early theory, proposed by Newcomb et al.,10[a] posited that there are two different oxidants – an ironoxo species and an iron-hydroperoxo species – which insert O and OH^+, respectively, into the C–H bond in a concerted fashion. This idea was suggested to explain how P450s could furnish both radical- and cation-derived products. However, computational studies by Shaik, Thiel, and coworkers[22] predict that the iron-hydroperoxo oxidant has insufficient reactivity to effect C–H hydroxylation.

22. Shaik, S.; Cohen, S.; Wang, Y.; Chen, H.; Kumar, D.; Thiel, W. P450 enzymes: their structure, reactivity, and selectivity—modeled by QM/MM calculations.*Chem. Rev.***2010**, *110*, 949.

23. (a) Ogliaro, F.; de Visser, S. P.; Cohen, S.; Sharma, P. K.; Shaik, S. Searching for the second oxidant in the catalytic cycle of cytochrome P450: a theoretical investigation of the iron(III)-hydroperoxo species and its epoxidation pathways.*J. Am. Chem. Soc.***2002**, *124*, 2806. (b) Meunier, B.; de Visser, S. P.; Shaik, S. Mechanism of oxidation reactions catalyzed by cytochrome P450 enzymes.*Chem. Rev.***2004**, *104*, 3947.(c) Newcomb, M.; Le Tadic, M.-H.; Putt, D. A.; Hollenberg, P. F. An incredibly fast apparent oxygen rebound rate constant for hydrocarbon hydroxylation by cytochrome P-450 enzymes.*J. Am. Chem. Soc.***1995**, *117*, 3312. (d) Newcomb, M.; Le Tadic-Biadatti, M.-H.; Chestney, D. H.; Roberts, E. S.; Hollenberg, P. F. *J. Am. Chem. Soc.* **1995**, *117*, 12085. (e) Newcomb, M.; Toy, P. H. Hypersensitive radical probes and the mechanisms of cytochrome P450-catalyzed hydroxylation reactions.*Acc. Chem. Res.***2000**, *33*, 449.

24. (a) Jin, S.; Makris, T. M.; Bryson, T. A.; Sligar, S. G.; Dawson, J. H. Epoxidation of olefins by hydroperoxo–ferric cytochrome P450.*J. Am. Chem. Soc.***2003**, *125*, 3406. (b) Vaz, A. D.; McGinnity, D. F.; Coon, M. J. Epoxidation of olefins by cytochrome P450: evidence from site-specific mutagenesis for hydroperoxo-iron as an electrophilic oxidant.*Proc. Natl. Acad. Sci. U. S. A.***1998**, *95*, 3555. (c) Vaz, A. D.; Pernecky, S. J.; Raner, G. M.; Coon, M. J. Peroxo-iron and oxenoid-iron species as alternative oxygenating agents in cytochrome P450-catalyzed reactions: switching by threonine-302 to alanine mutagenesis of cytochrome P450 2B4. *Proc. Natl. Acad. Sci. U. S. A.***1996**, *93*, 4644. (d) de Visser, S. P.; Ogliaro, F.; Harris, N.; Shaik, S. Multi-state epoxidation of ethene by cytochrome P450: a quantum chemical study. *J. Am. Chem. Soc.***2001**, *123*, 3037.

25. Shaik, S.; Cohen, S.; de Visser, S. P.; Sharma, P. K.; Kumar, D.; Kozuch, S.; Ogliaro, F.; Danovich, D. The "rebound controversy": an overview and theoretical modeling of the rebound step in C–H hydroxylation by cytochrome P450.*Eur. J. Inorg. Chem.* **2004**, 207.

26. Yang, Z.; Houk, K. N. The dynamics of chemical reactions: atomistic visualizations of organic reactions, and homage to van 't Hoff.*Chem. Eur. J.***2018**, *24*, 3916.

27. For an example of enzymatic control over reaction trajectories revealed by molecular dynamics trajectory simulations, see: Yang, Z.; Yang, S.; Yu, P.; Li, Y.; Doubleday, C.; Park, J.; Patel, A.; Jeon, B.; Russell, W. K.; Liu, H.; Russell, D. H.; Houk, K. N. Influence of water and enzyme SpnF on the dynamics and energetics of the ambimodal [6+4]/[4+2] cycloaddition. *Proc. Natl. Acad. Sci. U. S. A.***2018**,*115*, E848.

28. In solution, the energy surface for hydroxylation would be expected to lie somewhere in between the two extremes depicted in Figures 3a and 3b. The solvent cage would impose some local constraints, hampering the dissociation of the incipient radical [R•…(HO)Fe], but perhaps not as tightly as an enzyme active site. This scenario is relevant to C–H activation reactions catalyzed by synthetic mimics of cytochrome P450s.

29. Computations on the LS and HS energy surfaces are generally found to differ significantly only after the reorientation phase.[23]

30. (a) Elenewski, J. E.; Hackett, J. C.*Ab initio* dynamics of the cytochrome P450 hydroxylation reaction.*J. Chem. Phys.***2015**, *142*, 064307. For earlier MD simulations on a related hydroxylation reaction, see: (b) Yoshizawa, K.; Kamachi, T.; Shiota, Y. A theoretical study of the dynamic behavior of alkane hydroxylation by a compound I model of cytochrome P450.*J. Am. Chem. Soc.***2001**, *123*, 9806. For related MD simulations on MMO-catalyzed hydroxylation, see: Guallar, V.; Gherman, B. F.; Miller, W. H.; Lippard, S. J.; Friesner, R. A. Dynamics of alkane hydroxylation at the non-heme diiron center in methane monooxygenase.*J. Am. Chem. Soc.***2002**, *124*, 3377.

31. These ideas bear some relationship to an earlier model of concerted O insertion proposed by Newcomb and co-workers[23d] involving a side-on approach of the ferryl oxygen to the C–H bond.
32. Individual trajectories for a given reaction can display a broad range of time gaps ranging from dynamically concerted to dynamically stepwise. For example, the time gap for a di-π-methane rearrangement was shown to vary from 13 to 1160 fs depending on which vibrational modes were thermally activated in the TS. See: Jiménez-Osés, G; Liu, P.; Matute, R. A.; Houk, K. N. Competition between concerted and stepwise dynamics in the triplet di-π-methane rearrangement.*Angew. Chem. Int. Ed.***2014**, *53*, 8664.
33.Atkinson, J.K.; Ingold, K. U. Cytochrome P450 hydroxylation of hydrocarbons: variation in the rate of oxygen rebound using cyclopropyl radical clocks including two new ultrafast probes. *Biochemistry***1993**, *32*, 9209.
34. Cryle, M. J.; Hayes, P. Y.; De Voss, J. J. Enzyme–substrate complementarity governs access to a cationic reaction manifold in the $P450_{BM3}$-catalysed oxidation of cyclopropyl fatty acids. *Chem. Eur. J.***2012**, *18*, 15994.
35. He, X.; Ortiz de Montellano, P. R. Radical rebound mechanism in cytochrome P-450-catalyzed hydroxylation of the multifaceted radical clocks α-and β-thujone. *J. Biol Chem.***2004**,*279*, 39479.
36. (a) Bell, S. G.; Zhou, R.; Yang, W.; Tan, A. B.; Gentleman, A. S.; Wong, L. L.; Zhou, W. Investigation of the substrate range of CYP199A4: modification of the partition between hydroxylation and desaturation activities by substrate and protein engineering. *Chem. Eur. J.***2012**, *18*, 16677; (b) Wong, S. H.;Bell, S. G.; De Voss, J. J. P450 catalysed dehydrogenation.*Pure. Appl. Chem.***2017**, *89*, 841.

TOC graphic

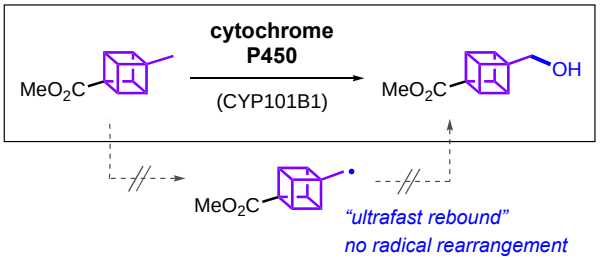
cytochrome
P450
(CYP101B1)
MeO2C
MeO2C
OH
MeO2C
"ultrafast rebound"
no radical rearrangement